Published in final edited form as:

Neuron. 2018 June 06; 98(5): 992–1004.e4. doi:10.1016/j.neuron.2018.04.030.

Hippocampal 5-HT input regulates memory formation and Schaffer collateral excitation

Catia M Teixeira[#1,2,8], **Zev B Rosen**[3,‡], **Deepika Suri**[1], **Qian Sun**[3], **Marc Hersh**[1], **Derya Sargin**[4,‡‡], **Iva Dincheva**[1,2], **Ashlea A. Morgan**[1], **Stephen Spivack**[1], **Anne C. Krok**[1,2], **Tessa Hirschfeld-Stoler**[1], **Evelyn K Lambe**[4,5,6], **Steven A Siegelbaum**[3,7], and **Mark S Ansorge**[1,2,9]

[1]Department of Psychiatry, Columbia University, New York, NY 10032.

[2]New York State Psychiatric Institute, New York, NY 10032.

[3]Department of Neuroscience, Kavli Institute, Vagelos College of Physicians and Surgeons, Columbia University 3227 Broadway, New York, New York 10027, USA

[4]Department of Physiology, University of Toronto, Toronto, Ontario M5S 1A8, Canada.

[5]Department of Obstetrics and Gynaecology, University of Toronto, Toronto, Ontario M5S 1A8, Canada

[6]Department of Psychiatry, University of Toronto, Toronto, Ontario M5S 1A8, Canada

[7]Department of Pharmacology, Vagelos College of Physicians and Surgeons, Columbia University

[8]Emotional Brain Institute, Nathan Kline Institute, Orangeburg, NY10962

[#] These authors contributed equally to this work.

Summary

The efficacy and duration of memory storage is regulated by neuromodulatory transmitter actions. While the modulatory transmitter serotonin (5-HT) plays an important role in implicit forms of memory in the invertebrate *Aplysia*, its function in explicit memory mediated by the mammalian hippocampus is less clear. Specifically, the consequences elicited by the spatio-temporal gradient of endogenous 5-HT release are not known. Here we applied optogenetic techniques in mice to gain insight into this fundamental biological process. We find that activation of serotonergic terminals in the hippocampal CA1 region both potentiates excitatory transmission at CA3-to-CA1 synapses and enhances spatial memory. Conversely, optogenetic silencing of CA1 5-HT terminals

[9]Corresponding author & Lead Contact: ma2362@cumc.columbia.edu.

[‡]Present address: Dr. Zev Rosen, Picower Institute for Learning and Memory, Department of Brain and Cognitive Sciences, MIT, Cambridge, MA02139

[‡‡]Present address: Dr. Derya Sargin, Hotchkiss Brain Institute and theDepartment of Physiology and Pharmacology, University of Calgary, Calgary, AB, Canada

Author Contributions

Conceptualization, M.S.A., C.M.T., S.A.S., Z.B.R.; Methodology, C.M.T., Z.B.R., Q.S., D.S., M.S.A.; Formal analysis, C.M.T., Z.B.R., Q.S., D.S., I.D., A.A.M., S.S., M.S.A.; Investigation, C.M.T., Z.B.R., D.S., Q.S., M.H., D.S., I.D., A.A.M., A.C.K., T.H.S., M.S.A.; Writing - Original Draft, C.M.T., Z.B.R., M.S.A.; Writing - Review & Editing, C.M.T., Z.B.R., D.S., Q.S., M.H., D.S., I.D., A.A.M., S.S., A.C.K., T.H.S., E.K.L., S.A.S., M.S.A.; Supervision, M.S.A., S.A.S., E.K.L.; Funding Acquisition, M.S.A, S.A.S., E.K.L.

Declaration of Interests

The authors declare no competing financial interest.

inhibits spatial memory. We furthermore find that synaptic potentiation is mediated by 5-HT4 receptors, and that systemic modulation of 5-HT4 receptor function can bidirectionally impact memory formation. Collectively, these data reveal powerful modulatory influence of serotonergic synaptic input on hippocampal function and memory formation.

Introduction

Learning and memory models suggest that modulation by subcortical inputs may stabilize Hebbian homosynaptic plasticity to permit long lasting changes in synaptic strength, and that these dynamic changes are the substrates for learning and memory (Bailey et al., 2000; Hunt et al., 2013). Monoamines - predominantly serotonin (5-HT), dopamine and norepinephrine - constitute the main class of subcortical modulatory input to higher brain regions involved in learning and memory. Recent studies demonstrate that local release of dopamine in the hippocampus plays a critical role in hippocampal-dependent learning and memory (Kempadoo et al., 2016; Rosen et al., 2015; Takeuchi et al., 2016). Although 5-HT is the prototypical modulatory neurotransmitter regulating sensitization and associative learning in the marine snail *Aplysia* (Bailey et al., 2000), relatively little is known about the role of 5-HT in memory formation in mammals.

Interestingly, the hippocampus, a mammalian brain region essential for declarative memory formation (Milner et al., 1998), receives dense serotonergic input from the raphe nuclei, which send fibers to the interface of the stratum radiatum (SR) and the stratum lacunosum-moleculare (SLM) layers in the CA1 area (Ihara et al., 1988). This site of innervation may enable 5-HT release to modulate both the direct entorhinal cortex input to CA1 via the perforant path (PP), and the indirect inputs that arrive in CA1 via the Schaffer collaterals (SC) from CA3. Both pathways undergo long-term potentiation (LTP) in response to tetanic stimulation, a form of plasticity thought to be important for memory formation (Basu and Siegelbaum, 2015; Gruart et al., 2006; Pastalkova et al., 2006; Tsien et al., 1996; Whitlock et al., 2006) and both pathways are necessary for optimal memory formation (Brun et al., 2002; Nakashiba et al., 2008; Suh et al., 2011).

However, there is conflicting evidence as to the role of 5-HT in hippocampal memory formation. Although bath-applied 5-HT agonists and inhibitors of 5-HT reuptake (SSRIs) can alter hippocampal plasticity (Cai et al., 2013; Cooke et al., 2014; Rubio et al., 2013), most studies report inhibitory effects of 5-HT on long-term potentiation or excitatory transmission (Corradetti et al., 1992; Jahnsen, 1980; Ropert, 1988; Staubli and Otaky, 1994). A positive role of 5-HT in memory is implied by the findings that cognitive deficits associated with depression or after tryptophan depletion are associated with reduced 5-HT levels (Cowen and Sherwood, 2013; Mendelsohn et al., 2009). However, systemically applied drugs that increase 5-HT signaling largely impair memory consolidation (Almeida et al., 2010; Gray and Hughes, 2015). Finally, 5-HT receptor subtype-specific compounds and mouse knockouts implicate the 5-HT1A, 5-HT3 and 5-HT4 receptors in regulating memory formation (Meneses, 2013; Ogren et al., 2008). While these studies demonstrate principal modulatory aspects of 5-HT on hippocampal function and learning and memory, there has been no direct examination of the effects of evoked 5-HT release from the serotonergic

inputs to the hippocampus. Here we investigate the consequences of optogenetic alteration of 5-HT release from genetically-defined serotonergic neurons on the physiological properties of CA1 pyramidal neurons, and on cognitive performance in a hippocampus-dependent spatial memory test.

Results

Light-induced regulation of serotonergic neuronal activity using ePet1-cre;Ai32 mice.

We first established a mouse line that expresses a channelrhodopsin2-enhanced green fluorescent fusion protein (ChR2-eYFP) exclusively in serotonergic neurons. To this end, we combined the *RC::LSL-CHR2* allele, which consists of conditional floxed *ChR2-eYFP* targeted to the *ROSA26* locus and will here be abbreviated as "*Ai32*" (Madisen et al., 2012), with the transgenic *B6.Cg-Tg(Fev-cre)1Esd/J* allele, which expresses Cre-recombinase under the *pet1* promoter and will here be abbreviated as "*ePet1-cre*" (Scott et al., 2005). ePet1-cre;Ai32 mice display YFP immunoreactivity (YFP+) in 5-HT immunopositive (5-HT +) neurons in the brainstem (Fig. 1a), with high specificity (99.5+/−0.2% 5-HT+/YFP+) and high transgene efficacy (95.3+/−1.1% YFP+/5-HT+; Fig. 1b, c). Serotonergic fibers labeled with YFP immunoreactivity were observed throughout the hippocampal region, with the highest local density found at the border of SLM and SR (Fig. 1d).

Photostimulation (10-ms long pulses of 473 nm light) at a frequency of 2 or 20 Hz increased the firing frequency of raphe serotonergic neurons in acute coronal brain slices of ChR2 expressing ePet1-cre$^{+/-}$;Ai32$^{+/+}$ but not ePet1-cre$^{-/-}$;Ai32$^{+/+}$ control mice (Frequency × Genotype interaction; $F_{(1, 43)} = 362.19$, $p<0.001$). Serotonergic neurons in the dorsal raphe (DR) and median raphe (MR) fired action potentials at a frequency that closely matched the pattern of photostimulation (Fig. 2b, f; for representative recordings see fig S1). *In vivo* optogenetic stimulation of ChR2-expressing mice through an optical fiber implanted in the DR or MR induced hyperlocomotion in the open field test (OF) (Fig. 2d, h) (Genotype × Stimulation interaction, DR: $F_{(8, 216)} = 5.214$; $p < 0.001$; MR: $F_{(8, 280)} = 5.124$; $p < 0.001$), demonstrating the *in vivo* efficacy of our approach.

Evoked terminal release of 5-HT in CA1 potentiates CA3 to CA1 inputs.

To study the effect of photostimulated release of 5-HT on hippocampal function, we next performed whole cell recordings from CA1 pyramidal cells in acute horizontal brain slices, with inhibition intact (Fig. 3a). Consistent with a previous report (Varga et al., 2009), we found a small, transient hyperpolarization of CA1 pyramidal neurons of 0.63 ± 0.11 mV in response to photostimulation at 2 Hz ($t_{(13)} = 5.617$; $p < 0.001$), which increased to a 1.12 ± 0.19 mV hyperpolarization ($t_{(13)} = 6.054$; $p < 0.001$) upon photostimulation at 20 Hz (Fig. 3b). This hyperpolarization was abolished by a cocktail of 5-HT receptor 1A, 3, and 4 antagonists (2 Hz ACSF vs 5-HT receptor block: $t_{(16)} = 2.534$; $p = 0.0221$; Fig. 3b).

Next, we investigated whether 5-HT release altered synaptic excitation of the CA1 pyramidal neurons by either their SC or PP inputs (Fig. 4a, d). We electrically stimulated the SR of CA1 at 0.05 Hz to evoke a SC-mediated fast postsynaptic potential (PSP) in CA1 pyramidal neurons (PNs). After 5 minutes of baseline recording, we delivered 50 light pulses

at 2 Hz. Optogenetic activation of serotonergic terminals increased the amplitude of the SC-evoked PSP in CA1 PNs by 96 ± 26% (One-way RM ANOVA: $F_{(2.49, 17.42)} = 5.35$, p = 0.0114; Fig. 4b–c; extended holding see fig. S2b). Photostimulation had no effect on the SC-evoked PSP in ePet1-cre$^{-/-}$;Ai32$^{+/+}$ control mice (fig. S2c–d). Bath application of the 5-HT receptor antagonist cocktail abolished the optogenetically-induced potentiation (treatment × time interaction: two-way RM ANOVA: $F_{(20, 200)} = 2.403$, p = 0.0011; 5-HT receptor block: one-way RM ANOVA: $F_{(2.016, 6.048)} = 1.208$, p = 0.3623; Fig. 4b–c). In contrast, optogenetic release of 5-HT did not alter the PP-evoked PSPs in CA1 pyramidal neurons (One-way RM ANOVA: $F_{(3.2, 22.41)} = 0.4731$, p = 0.4731, Fig. 4e–f). Together these data demonstrate serotonergic potentiation of the CA3 to CA1 (SC) but not EC to CA1 (PP) inputs upon optogenetic stimulation of serotonergic axons in CA1.

The enhancement in the SC-evoked PSP could reflect an increase in the excitatory postsynaptic current (EPSC), a decrease in feedforward inhibition, or an increase in dendritic integration of the EPSC. To distinguish among these possibilities, we examined the effect of optogenetic 5-HT release on the extracellular field EPSP, whose amplitude is proportional to the local EPSC. We electrically stimulated the SR of CA1 at 0.05 Hz to evoke a SC-mediated, fast, excitatory postsynaptic field potential (fEPSP) in CA1 (Fig. 4g). After 5 minutes of baseline recording, we delivered 50 light pulses at 20 Hz. Optogenetic activation of serotonergic terminals increased the amplitude of the SC-evoked fEPSP in CA1 PNs by 117 ± 40% (One-way RM ANOVA: $F_{(1.229, 6.143)} = 4.883$, p = 0.064; Fig. 4h–i), similar to the effect on the intracellular PSP. Direct evidence that the potentiation does not reflect a decrease in inhibition is provided by experiments using GABA antagonists presented below (see Figs. 7 and S8b).

Next, we investigated if serotonergic fEPSP potentiation occurs *in vivo* (Fig. 4k). We targeted optical stimulation to the cell bodies of serotonergic neurons, because acute penetration of the CA1 PN layer with the optical fiber disrupts LFP responses to electrical stimulation of SC (data not shown). We positioned the optical fiber in the MR, where we find the serotonergic neurons reside that project to CA1 (Fig. S7a–c). We electrically stimulated SCs at 0.2 Hz to evoke fast, excitatory postsynaptic field potentials (fEPSP) in dorsal CA1 of anesthetized mice. On its own, this protocol did not elicit potentiation or depression of fEPSP responses (One-way RM ANOVA: $F_{(1.686, 30.34)} = 2.287$, p = 0.1261; Fig. S2e–g) (Huang et al., 2004). To test for an effect of neurotransmitter release from serotonergic neurons on fEPSPs *in vivo*, we delivered 50 light pulses at 20 Hz after 5 minutes of baseline recording. Optogenetic activation of serotonergic neurons increased the amplitude of the SC-evoked fEPSP in CA1 PNs by 40 ± 9% (One-way RM ANOVA: $F_{(1.409, 43.68)} = 14.03$, p = 0.0001; Fig. 4h–i).

Optogenetic stimulation of serotonergic axons in CA1 increases spatial memory formation.

Next, we studied the consequences of optogenetically stimulating serotonergic neurons on spatial memory using the Morris water maze test (MWM) (Teixeira et al., 2006) (fig. S3a, f). We hypothesized that 5-HT release may enhance spatial memory storage given the potentiation of CA3-CA1 synaptic excitation observed both in acute hippocampal slices as

well as in anesthetized mice. Hence, we first subjected mice to a weak training protocol (fig. S3b, g). ChR2-expressing mice and their littermate controls with optical fiber implants in the DR or MR were trained in the MWM for 5 days using 3 trials per day, with continuous photostimulation during training (473 nm, 20Hz, 10ms, 10mW). Mice improved their performance during training, measured as a decreased latency to find the platform (DR: $F_{(4,104)} = 32.044$; $p < 0.0001$; MR: $F_{(4,128)} = 29.981$; $p < 0.0001$; fig. S3c, h). Spatial memory was assessed in a probe trial in which the platform was removed without photostimulation. We did not detect an effect of genotype or implant location on probe trial performance (fig. S3d, e, i, j).

We hypothesized that the hyperlocomotion phenotype observed with raphe stimulation (Fig. 2d, h) might interfere with attention-related aspects important for memory formation and might be elicited by neurotransmitter release in non-hippocampal serotonergic projection fields. Hence, we next used a protocol to selectively activate serotonergic input into the hippocampus, and specifically to the dorsal CA1, by implanting optical fibers targeting the SLM/SR border (Fig. 5a; fig. S4a). Optogenetic stimulation of serotonergic fibers in dorsal CA1 had no effect on locomotor activity ($OF_{distance}$: Genotype × Stimulation interaction: $F_{(11, 341)} = 1.10$; $p = 0.3607$; Fig. 5b). In the MWM, both groups of mice equally improved their performance during training (Training day effect: $F_{(4,72)} = 11.32$; $p < 0.0001$; Fig. 5g). However, in the probe trial that tests memory retrieval ChR2-expressing mice spent significantly more time in the target zone of the pool (where the platform was located) than their littermate controls or the average of the three non-target zones (Search zone × Genotype interaction: $F_{(1, 18)} = 8.033$; $p = 0.0110$; Fig. 5h). Furthermore, ChR2 mice showed significantly more platform crossings than their littermate controls ($t_{(18)}=2.054$; $p=0.0274$; Fig. 5i), suggesting that serotonergic terminal stimulation in dorsal CA1 improved cognition.

In contrast to memory retrieval, we did not detect a Genotype × Stimulation effect on behavior in the OF or Forced-Swim-Test (FST) (Fig. 5c–d) ($OF_{CenterTime}$: Genotype × Stimulation interaction: $F_{(11, 341)} = 1.23$; $p = 0.2685$. FST: Genotype × Stimulation interaction: $F_{(11, 319)} = 1.08$; $p = 0.3755$). For tests with alternating light-off and light-on conditions we performed an additional analysis, grouping all light-off bins and all light-on bins. Again, no significant Genotype × Stimulation interactions were detected ($OF_{Distance}$: Genotype × Stimulation interaction: $F_{(1, 31)} = 2.973$; $p = 0.0946$. $OF_{CenterTime}$: Genotype × Stimulation interaction: $F_{(1, 31)} = 0.027$; $p = 0.87$. FST: Genotype × Stimulation interaction: $F_{(1, 29)} = 2.639$; $p = 0.1151$). Hence performance in the MWM was not confounded by alterations in ambulatory activity, anxiety-like behavior or swimming behavior. Also, the improvement in memory was specific to spatial learning, as ChR2-mediated stimulation did not affect performance in a social memory recognition task (Treatment × Mouse Novelty effect: $F_{(3, 60)} = 1.03$; $p = 0.3874$. Mouse novelty effect: $F_{(1, 60)} = 47.81$; $p < 0.0001$; Fig. 5e), which is dependent on the CA2 region (Hitti and Siegelbaum, 2014).

To control for unspecific effects of genotype or off target activation, we performed several additional control experiments. First we confirmed that ChR2 expression in serotonergic neurons without light stimulation did not affect behavior in any test we performed (fig. S5c–j). Second, we investigated whether light traveling through the targeted CA1 region might

reach the dentate gyrus (DG) to excite local serotonergic axon terminals of this upstream hippocampal subfield to produce observed behavioral effects. To address this possibility, we selectively activated serotonergic input into the dorsal DG by implanting optical fibers targeting its outer blade (fig. S4c). Optogenetic stimulation of serotonergic fibers in the dorsal DG had no effect on MWM behavior (fig. S6). Both groups of mice equally improved their performance during training (Training day effect: $F_{(4,96)} = 12.329$; $p < 0.0001$; fig. S6c). Likewise, in the probe trial, no Search Zone by Genotype interaction was detected ($F_{(1,24)} = 1.296$; $p = 0.2662$; fig. S6d). Furthermore, ChR2 mice did not differ significantly from littermate controls for platform crossings ($F_{(1,24)} = 0.882$; $p = 0.357$; fig. S6e), demonstrating that serotonergic terminal stimulation in the dorsal DG does not impact spatial memory formation in the MWM.

One potential concern with in vivo stimulation of serotonergic axons in dorsal CA1 is that it is expected to trigger antidromic action potentials, which could travel back to the raphe and excite collaterals that release 5-HT in other brain regions. We therefore directly assessed whether local optogenetic stimulation of serotonergic axons in hippocampus is able to excite serotonergic neurons in the raphe. As raphe neuron activation has been found to induce immediate early gene *c-Fos* expression (Ahmari et al., 2013; Teissier et al., 2015; Veerakumar et al., 2014), we examined Fos staining in the raphe following optical stimulation in dorsal CA1 (fig. S7). To maximize our sensitivity of detecting activation, we first mapped the raphe region that contains serotonergic neurons projecting to the dorsal CA1 region. To that end, we injected a retrograde Cre-dependent CAV2 virus conditionally expressing ZsGreen (Sanford et al., 2017) into dorsal CA1. We detected retrogradely labeled serotonergic neurons exclusively in MR (fig. S7c) and hence restricted our analysis to this raphe sub-region. We failed to detect an effect of hippocampal serotonergic photostimulation in enhancing Fos staining in 5-HTergic MR neurons compared to controls (no effect of genotype; $t_{(1,4)} = 4.514$; $p = 0.1008$; fig. S7g). However, direct optical stimulation of MR 5-HTergic neurons enhanced 5-HTergic Fos reactivity compared to controls ($t_{(1,4)} = 6.662$; $p = 0.0026$; fig. S7l). Together, these data indicate that stimulation of raphe projections in dorsal CA1 did not antidromically activate serotonergic neurons in the raphe. Thus, any behavioral effects of optogenetic activation likely reflect local actions of 5-HT release within CA1. Further support for a local role of 5-HT in hippocampus comes from optogenetic inhibition experiments, discussed next.

Optogenetic inhibition of serotonergic axons in CA1 reduces spatial memory formation.

Does endogenous serotonergic activity in CA1 normally contribute to memory formation? To examine this question, we expressed the light-gated proton pump Archaerhodopsin (Arch), which inhibits neural activity upon photostimulation, in serotonergic neurons by crossing ePet1-cre mice to the *RC::LSL-Arch* line, which consists of conditional floxed *Arch-eYFP* targeted to the *ROSA26* locus and will here be abbreviated as "*Ai35*" (Madisen et al., 2012). Arch expressing mice (ePet1-cre+/−;Ai35+/+) and their littermate control mice (ePet1-cre−/−;Ai35+/+) were implanted with a fiber optic probe targeting the CA1 SLM/SR border (Fig. 6a; fig. S4b). Mice were initially trained in the MWM for 6 days (3 trials a day), with continuous photostimulation during training on days 4–6 (532 nm, 10mW) (Fig. 6f). Both groups of mice improved performance as the test progressed (effect of time for D1-D6:

$F_{(5, 85)} = 10.262$; $p < 0.001$; Fig. 6g). In a subsequent probe trial without light stimulation, both groups of mice showed comparable low levels of performance (Zones × Genotype: $F_{(1, 17)} = 0.007$; $p = 0.9343$. Zones: $F_{(1, 17)} = 4.267$; $p = 0.0545$. Platform crossings: $t_{(17)} = 0.4037$; $p = 0.6915$; Fig. 6i). To increase spatial reference memory and avoid a possible floor-effect, we trained mice for 3 additional days with light stimulation, which further improved their performance (effect of time for D6-D9: $F_{(3, 51)} = 4.946$; $p = 0.0043$; Fig. 6g). In a subsequent second probe trial (P2), we found that the Arch-expressing mice exposed to photostimulation during training now showed a significant impairment in memory during the probe trial compared to control littermates. We detected a trend for Search Zone by Genotype interaction (Zones × Genotype: $F_{(1, 17)} = 4.170$; $p = 0.057$), with control mice spending more time in the Target zone than in the Other zones, while Arch mice showed no preference (Fig. 6h). We also detected an interaction of probe trial performance and genotype ($F_{(1, 17)} = 4.7$; $p = 0.0447$) as well as a genotype effect for platform crossings on P2 ($t_{(17)} = 0.2509$; $p = 0.0225$), with control mice showing 65.4% more platform crossings than Arch mice (Fig. 6i). These data demonstrate a decrease in cognitive performance when serotonergic cell signaling is inhibited during training. Arch mice did not differ from controls in the OF ($OF_{distance}$: Genotype × Stimulation interaction: $F_{(11, 286)} = 1.738$; $p = 0.0648$. $OF_{CenterTime}$: Genotype × Stimulation interaction: $F_{(11, 286)} = 0.703$; $p = 0.7356$), FST (Genotype × Stimulation: $F_{(11, 308)} = 0.376$; $p = 0.9647$) or social memory recognition task (Treatment × Mouse Novelty interaction: $F_{(3,12)} = 0.20$; $p = 0.8946$) (Fig. 6b–e). For tests where we alternated light-off and light-on conditions we performed an additional analysis, grouping all light-off bins and all light-on bins. Again, no significant Genotype × Stimulation interactions were detected ($OF_{Distance}$: Genotype × Stimulation interaction: $F_{(1, 26)} = 0.046$; $p = 0.8322$. $OF_{CenterTime}$: Genotype × Stimulation interaction: $F_{(1, 26)} = 0.156$; $p = 0.6957$. FST: Genotype × Stimulation interaction: $F_{(1, 28)} = 0.656$; $p = 0.4246$).

5-HT elicited synaptic potentiation of CA3-to-CA1 inputs is mediated by 5-HT4 receptors.

To investigate the extent to which the electrophysiological and behavioral effects of 5-HT release may be related, we studied the role of specific 5-HT receptors in these actions. The acute transient hyperpolarization of CA1 pyramidal neurons is blocked by the 5-HT receptor antagonist cocktail (Fig. 3b) and by 5-HT1AR blockade alone ($t_{(4)} = 3.587$; $p = 0.6527$; Fig. 7a). However, the effect is not altered by either a 5-HT4R antagonist ($t_{(9)} = 3.587$; $p = 0.0059$) or by blocking $GABA_A$ and $GABA_B$ receptors ($t_{(7)} = 3.674$; $p = 0.0079$) (Fig. 7a). This result is consistent with findings that photostimulation of the MR to CA1 projections in the rat induces a 5-HT1A receptor dependent hyperpolarization of CA1 pyramidal cells (Varga et al., 2009). Conversely, the potentiation of the SC CA3-CA1 synapse is blocked by the 5-HT receptor antagonist cocktail (Fig. 4b, c) and by a 5-HT4R antagonist alone (treatment X time interaction: two-way RM ANOVA: $F_{(20, 200)} = 3.658$, $p < 0.001$, Fig. 7b) but is not affected by 5-HT1AR blockade (+150±45%, baseline vs. last 5 minutes: $t_{(3)} = 3.324$; $p = 0.0449$, 5-HT1AR blockade vs. ACSF: $t_{(9)} = 1.793$; $p = 0.063$, Fig. 7c), or GABA receptor blockade (+185±22%, baseline vs. last 5 minutes: $t_{(9)} = 3.881$; $p = 0.0037$, GABA blockade vs. ACSF: $t_{(17)} = 1.506$; $p = 0.17$, Fig. 7c, fig. S8a). The 5-HT4R antagonist fully blocked the PSP potentiation upon photostimulation with either a 20 Hz train (One-way RM ANOVA: $F_{(20, 84)} = 0.5058$, $p = 0.9572$; Fig. 7b,c) or a 2 Hz train (One-way RM ANOVA: $F_{(3.28, 19.69)} = 1.372$, $p = 0.2806$, fig. S8b; Fig. 7c). We next investigated if the CA3-CA1

potentiation is expressed pre- or postsynaptically. To address this question, we examined the paired-pulse ratio before and after optical stimulation, as a measure of presynaptic function. We did not detect a significant effect of photostimulated 5-HT release in whole-cell ($t_{(16)}$ = 0.9795; p = 0.3419, Fig. 7d) or field (One-way RM ANOVA: $F_{(4.387, 21.93)}$ = 1.555, p = 0.2187, Fig. 7e) recordings, suggesting that the effect is mediated postsynaptically through 5-HT4 receptors on CA1 pyramidal neurons (Penas-Cazorla and Vilaro, 2015). In further support of a postsynaptic mechanism, we find cell-intrinsic changes in patched PNs in response to optogenetic neurotransmitter release from serotonergic axons, with input resistance increasing by ~15% (n = 8, p = 0.0201; Fig. 7f).

Bidirectional modulation of memory formation through systemic administration of drugs targeting 5-HT4 receptors.

To determine the importance of 5-HT4R activation in spatial learning, we examined the effect of systemic administration of the specific antagonist GR125487 (10 mg/kg, i.p.) and agonist BIMU8 (30 mg/kg, i.p.) (Fig. 8). Injection of GR125487 prior to MWM training impaired probe trial performance, significantly decreasing platform crossings ($t_{(34)}$ = 2.064; p = 0.0467; Fig. 8d), but did not alter Search Zone preference (Zones × Genotype: $F_{(1, 34)}$ = 0.485; p = 0.4907; Fig. 8c). Conversely, BIMU8 injections prior to MWM training enhanced probe trial performance. We detected a trend for Search Zone by Genotype interaction (Zones × Genotype: $F_{(1, 17)}$ = 3.318; p = 0.0862), with BIM-treated mice spending more time in the Target zone than in the Other zones, while Saline-treated mice showed no preference (Fig. 8g). BIM-treated mice also significantly increased platform crossings while Saline-treated mice did not (probe trial × genotype interaction: $F_{(1, 17)}$ = 9.462; p = 0.0068 Fig. 4i). We also tested the effect of BIMU8 and GR125487 in the OF and FST. BIMU8 treatment significantly reduced ambulatory activity in the OF ($F_{(2, 46)}$ = 12.582; p < 0.0001, Fig. 8i), potentially complicating the interpretation of MWM behavior. However, center activity and FST behavior were not affected by BIMU8 treatment ($F_{(2, 46)}$ = 0.784; p = 0.4626, Fig. 8j; $F_{(2, 23)}$ = 0.173; p = 0.8422, Fig. 8k), suggesting that emotional behavior and swimming abilities do not confound MWM behavior. GR125487 treatment had no effect on OF or FST behavior (Fig. 8i–k). Together these data suggest that hippocampal 5-HT4R activation is both necessary for optimal memory formation and sufficient to enhance memory formation.

Discussion

Together, our data reveal that the serotonergic input to the hippocampal CA1 region participates in both potentiation of SC CA3-CA1 synaptic excitation and memory storage performance. Moreover, these effects appear to be mediated by the 5-HT4 receptor.

5-HT4 receptors signal through diverse G-protein-dependent and G-protein-independent pathways (Bockaert et al., 2011; Bockaert et al., 1990; Dumuis et al., 1988). Intriguingly, their canonical coupling to $G\alpha_s$ highlights a role of 5-HT in memory formation that potentially mirrors the cAMP-dependent facilitatory action of 5-HT on the sensory-to-motor neuron synapse in *Aplysia* (Brunelli et al., 1976; Kandel and Schwartz, 1982), suggesting a functional evolutionary conservation. However, whereas in Aplysia 5-HT acts on

presynaptic 5-HT receptors to enhance transmitter release, we find no effect of 5-HT release on the paired pulse ratio, suggesting that the CA3-CA1 potentiation is expressed postsynaptically.

Our results are consistent with an effect of 5-HT to directly enhance the SC glutamatergic EPSP. Thus, the 5-HT4 receptor-mediated potentiation occurs independently of GABA receptor activation. These data are in line with *Htr4* expression by CA1 pyramidal neurons and the lack of *Htr4* expression by CA1 GABAergic neurons (Andrade, 1998; Penas-Cazorla and Vilaro, 2015; Torres et al., 1996). Our findings are also congruent with transient pharmacologic 5-HT4 receptor activation producing persistent EPSP spike potentiation (Mlinar et al., 2006). Indeed, our whole-cell recordings revealed a small but significant increase in input resistance, indicating that cell intrinsic properties contribute to the potentiation of postsynaptic potentials, although the magnitude of the EPSP and fEPSP potentiation (100%) is too large to be solely accounted for by the change in resistance (15%). Future experiments will be useful in dissecting the relative contribution of alterations in synaptic strength compared to intrinsic excitability.

We also identified a 5-HT1A receptor-mediated fast, transient, GABA-independent hyperpolarization of CA1 pyramidal neurons. This result is consistent with findings that photostimulation of the MR to CA1 projections in the rat induces direct 5-HT1A receptor-dependent hyperpolarization of CA1 pyramidal cells (Varga et al., 2009). Importantly we found that the 5-HT4 receptor-mediated effect predominates, lasting for at least 30 minutes. This balance towards 5-HT4 receptor-mediated synaptic excitation was at first surprising, as we had originally hypothesized to find a dominant 5-HT1A receptor mediated inhibition, which had been suggested by *in vitro* work using bath application of serotonergic drugs (Corradetti et al., 1992; Jahnsen, 1980; Ropert, 1988; Staubli and Otaky, 1994). The contrasting outcome demonstrates the critical role that the spatio-temporal parameters of extracellular 5-HT distribution play in determining cell-physiological consequences, and emphasizes importance of optogenetic approaches to examine effects of release of endogenous modulatory transmitters (Rosen et al., 2015). Our findings are in line with 5-HT1A receptors being located predominantly at extra-synaptic and non-synaptic sites (Riad et al., 2000), where they participate in 5-HT volume transmission and might serve as inhibitory spill-over detectors. Additional 5-HT receptor genes are expressed in the hippocampus, including *Htr2a*, *Htr2C*, and *Htr7* (Tanaka et al., 2012), but their role has not been studied here. Consequently, we do not rule out that these receptors might also relay physiological information with behavioral consequences. Likewise, a partial GABA-dependence might be present and detectable with increased N.

We find no effect of photostimulated 5-HT release on synaptic excitation evoked by the direct entorhinal cortical input to CA1 pyramidal neurons. This dissociation suggests that 5-HT release in CA1 can selectively modulate the indirect versus the direct hippocampal pathway. Interestingly, 5-HT potentiates the temporoammonic-CA1 synapse in rat hippocampal slices after pharmacologic 5-HT transporter blockade (Cai et al., 2013). The discrepancy in outcome again likely relates to the spatio-temporal differences in extracellular 5-HT concentrations elicited by both serotonergic manipulations and points to its possible synapse selective allocation in changing experimental conditions.

Our finding that both 2 and 20 Hz optical stimulation of terminal 5-HT release are able to potentiate the SC CA3-CA1 synapse has important implications. Because serotonergic neurons fire at 2 – 20 Hz *in vivo* (Cohen et al., 2015; Liu et al., 2014; Wang et al., 2015), our findings suggest that potentiation of SC CA3-CA1 synapses likely occurs during physiological patterns of activity where it can contribute to a behavioral enhancement in spatial memory. This interpretation is supported by our control experiment, demonstrating that light spread to the DG does not contribute to the behavioral phenotype. Furthermore, we do not find evidence that terminal stimulation in CA1 activates serotonergic activity throughout the brain, while direct activation of serotonergic neurons at the cell body level in either the DR or the MR does not phenocopy CA1 terminal stimulation. Finally, CA1 terminal inhibition of serotonergic fibers produces the opposite behavioral phenotype, impairing spatial memory, demonstrating that endogenous serotonergic activity normally contributes to memory formation. While 5-HT is generally thought to be not sufficient to tonically activate postsynaptic receptors *in vivo* under baseline conditions in the hippocampus, our data are congruent with tonic coding properties of serotonergic neurons (Cohen et al., 2015) as well as 5-HT4 receptor antagonists impacting hippocampal physiology (Kemp and Manahan-Vaughan, 2005; Wawra et al., 2014).

Our pharmacological experiments also support a link between the action of 5-HT on the SC CA3-CA1 synapse and behavior, as we demonstrate bidirectional modulation of memory formation in the Morris water maze task through systemic stimulation or inhibition of 5-HT4 receptor signaling. By choosing a systemic approach we activate 5-HT4 receptors throughout the organism, and interaction with non-CA1 receptors can complicate the interpretation of the results. For example, we find 5-HT4 receptor agonism inhibits locomotion in the OF, while terminal manipulation of 5-HTergic activity in CA1 does not impact OF locomotion. Importantly systemic 5-HT4 receptor agonism did not impact swimming behavior, and we did not detect other consequences that would complicate our interpretation of MWM data. As for the locus of the effect on MWM behavior, we can likewise not conclude but only suggest a role of CA1 5-HT4 receptors. Hence our pharmacology experiments allow us to formulate hypotheses regarding necessity and sufficiency of 5-HT4 receptors present on CA1 pyramidal neurons that can be tested for example with conditional genetics. Importantly, our data are also informative in the context of pharmacotherapy.

Behavioral effects are by and large in line with the effects of global 5-HT depletion, which impairs memory performance (Hritcu et al., 2007; Matsukawa et al., 1997). However, global increases of 5-HT signaling through systemic SSRI treatment impairs Morris water maze performance (Majlessi and Naghdi, 2002) and short-term spatial memory in a Y maze (Gray and Hughes, 2015), indicating a more complex interaction between the effects of multiple 5-HT receptor subtypes. Research on 5-HT4 receptors is congruent with our findings, with 5-HT4 agonists improving olfactory discrimination performance (Restivo et al., 2008) and place/object recognition memory (Lamirault and Simon, 2001) and an antagonist impairing associative memory (Marchetti et al., 2000), as well as inhibiting low frequency stimulation-induced LTD in CA1 pyramidal neurons (Kemp and Manahan-Vaughan, 2005). Hence our data not only provide mechanistic insight into how serotonergic signaling pathways are recruited in the spatio-temporal context of circuit-specific terminal neurotransmitter release,

but also support the notion that serotonergic drugs targeting the 5-HT4 receptor may provide an effective means for modulating cognitive function.

STAR+METHODS

CONTACT FOR REAGENT AND RESOURCE SHARING

Further information and requests for reagents may be directed to, and will be fulfilled by, the Lead Contact and corresponding author, Dr. Mark Ansorge (ma2362@cumc.columbia.edu)

EXPERIMENTAL MODEL AND SUBJECT DETAILS

ePet1-cre (Scott et al., 2005), Ai32 and Ai35 (Madisen et al., 2012) female and male mice were maintained on a 129SvEv/Tac background at the Rodent Neurobehavioral Analysis Core at Columbia University or the University of Toronto. The ePet1-cre line was originally generated on the (C57BL/6 × SJL)F2 background and has been backcrossed in our lab to 129SvEv/Tac for >10 generations. The Ai lines were generated on the (129S6/SvEvTac × C57BL/6NCrl)F1 and have been backcrossed in our lab to 129SvEv/Tac for 6 generations. Double transgenic and their single transgenic littermate controls were housed in groups (two to five mice per cage) and maintained in a 12 h light/dark cycle with access to food and water ad libitum. Experiments were conducted blind and in compliance with the Principles of Laboratory Animal Care National Institute of Health (NIH) guidelines and the institutional animal committee guidelines. We used two groups of transgenic mice expressing different opsins (channelrodopsin2 or archaerodopsin) in serotonergic cells. For serotonergic cell activation we used two genotypes: ePet1-cre$^{+/-}$;Ai32$^{+/+}$ (ChR2) and ePet1-cre$^{-/-}$;Ai32$^{+/+}$ (Control). In some electrophysiological experiments mice heterozygous for Ai32 were used: ePet1-cre$^{+/-}$;Ai32$^{+/-}$ (ChR2) and ePet1-cre$^{-/-}$;Ai32$^{+/-}$ (Control). For serotonergic cell silencing we used ePet1-cre$^{+/-}$;Ai35$^{+/+}$ (Arch) and ePet1-cre$^{-/-}$;Ai35$^{+/+}$ (Control). Mice were tested at 3 – 6 months of age.

METHOD DETAILS

Drug Administration: For electrophysiology, the pharmacological agents were applied to the slice preparation by dissolving them in the perfused ACSF. Applied concentrations were: 5-HT4 antagonist, GR113808 (100 nM); 5-HT3 antagonist, odansetron (10 nM); 5-HT1A antagonist, WAY100635 (100 nM). These antagonists were chosen because they target 5-HT receptors that are prominently present in CA1 (see Allen Brain Atlas). The 5-HT receptor antagonist cocktail contained all three antagonists. GABA block was performed with the GABA-A receptor antagonist SR-95531 (2 μM) and the GABA-B receptor antagonist CGP-35348 (1 μM).

For the water maze, the 5-HT4 antagonist GR125487 was dissolved in 0.9% NaCl and administered intraperitoneally at 10 mg/kg 20min before training. The 5-HT4 agonist BIMU8 was dissolved in 0.9% NaCl and administered intraperitoneally at 30 mg/kg 20min before training.

Electrophysiological Recording and Analysis: For all raphe-related experiments, coronal brainstem slices including the dorsal or median raphe nuclei were sliced with a

Dosaka Pro 7 Linear Slicer (DSK) in sucrose-substituted ACSF. Electrophysiological recordings were performed in regular ACSF (in mM): 128 NaCl, 10 D-glucose, 26 $NaHCO_3$, 2 $CaCl_2$, 2 $MgSO_4$, 3 KCl, 1.25 NaH_2PO_4, pH 7.4 and saturated with 95% O_2/5% CO_2 at 31–33°C. To maintain 5-HT synthesis, 2.5 μM L-tryptophan was included during the recovery period. Patch pipettes contained the following (in mM): 120 potassium gluconate, 5 KCl, 2 $MgCl_2$, 4 K_2-ATP, 0.4 Na_2-GTP, 10 Na_2-phosphocreatine, and 10 HEPES buffer (adjusted to pH 7.3 with KOH). Neurons were visualized with a fixed-staged microscope (Olympus BX50WI) and 5-HT neurons were targeted based on the expression of eGFP. Whole-cell recordings were made in current-clamp mode with a Multiclamp 700B amplifier (Molecular Devices). All data were acquired at 20 kHz and low-pass filtered at 3 kHz using pClamp10.2 and Digidata1440 software. Analysis was performed using pClamp 10.2 software (Molecular Devices).

For whole-cell recordings, horizontal brain slices were prepared from the hippocampus of P49-P90 mice. Animals were anesthetized with isoflurane and then perfused intracardially with ice-cold (2°C) sucrose-replaced ACSF (S-ACSF) containing (in mM): NaCl (10), NaH_2PO_4 (1.2), KCl (2.5), $NaHCO_3$ (25), glucose (25), $CaCl_2$ (0.5), $MgCl_2$ (7), sucrose (190), pyruvate (2), continuously bubbled with 95%/5% O_2/CO_2. After decapitation and brain removal, brains were submerged in the S-ACSF and hemisected. The cerebellum and anterior portion of the brain were removed. The hemisected brain was then cut in the horizontal plane at a 10–12° angle in the ventromedial direction to optimally achieve a transverse section (perpendicular to the longitudinal axis of the hippocampus) and sliced into 400 μm-thick sections on a Leica VT1200s sectioning system. Slices between bregma distance −2.16 to −3.96 were then incubated in a 34°C solution consisting of 50% S-ACSF and 50% recording ACSF containing (in mM): NaCl (125), NaH_2PO_4 (1.25), KCl (2.5), $NaHCO_3$ (25), Glucose (25), $CaCl_2$ (2), $MgCl_2$ (1), pyruvate (2) for 20 minutes and then sat at room temperature until recording. When ready for recording, slices were placed into a submerged chamber in the rig at 30–32°C, and constantly supplied at 4–5 ml/minute with 95%/5% O_2/CO_2 R-ACSF.

Whole cell current clamp recordings were obtained from pyramidal neurons in CA1 using patch pipettes (3–5 MΩ) filled with $KMeSO_4$ (135), KCl (5), EGTA-Na (0.1), HEPES (10), NaCl (2), ATP (5), GTP (0.4), phosphocreatine (10) (pH of 7.2; 280–290 mOsm). Series resistance (typically 10–25 MΩ) was monitored throughout each experiment; recordings with a > 20% change in series resistance were excluded from analysis. Focal stimulating electrodes, lower resistance patch pipettes filled with R-ACSF, were used to apply unipolar shocks of 0.1 ms duration using a constant voltage stimulator. Recordings form CA1 PNs were performed using the both the visual and blind patch methods.

Recordings were obtained using a two-channel multiclamp 700B amplifier (Axon Instruments). Data were digitized on a PC using a Digidata 1440 interface under the control of the AxographX acquisition package (Berkeley, CA). Data were acquired at 20 kHz with a 10 kHz low-pass Bessel filter applied using the internal circuitry of the Multiclamp amplifier. Analysis was completed using AxographX software, MATLAB student version (Mathworks, Natick, MA), Excel (Microsoft, Redmond, WA), and Prism (GraphPad Software, La Jolla, CA).

Input resistance (Rin) was measured by injecting a −50 or −100 pA current pulse with a 500 ms duration. The amplitude of the voltage deflection was then measured and, via Ohm's law, Rin was calculated.

For PSP recordings, electrical stimulation was given once every 20s, a frequency that avoids any plasticity induction. The amplitude of synaptic responses was measured as a small windowed average of the peak potential following stimulation. Data were normalized to the average of the baseline 5 minutes before the manipulation and then box-car filtered such that each point represents the average of 3 points (1 minute each). The fold change was, therefore, the average magnitude of the PSP post-manipulation divided by the average magnitude of the baseline EPSP.

For extracellular field recordings, transverse hippocampal slices were prepared as described previously (Sun et al., 2014). Briefly, mice were anesthetized with isoflurane and sacrificed by decapitation. Hippocampi were dissected out, and transverse slices (400 μm thickness) were cut on a vibratome (Leica VT1200S, Germany) in ice-cold S-ACSF. The slices were then incubated at 33 °C in ACSF for 20–30 min and then kept at room temperature for at least 1.5 hours before transfer to the recording chamber. Field potentials were recorded with glass patch pipettes containing 1 M NaCl. The recording pipettes were placed in the middle of SR in CA1b area. Field responses were evoked using a stimulating electrode placed in the middle of SR of the CA1 field (~200 μm from the recording pipettes).

Optical stimulation was delivered using a 470-nm collimated blue LED (Thorlabs), which was mounted on the backport of the microscope and focused through the objective (Olympus, 40×, 0.8 N.A.) with the aperture opened for full-field illumination (3.50 mW mm $^{-2}$), and positioned over stratum radiatum.

In vivo recordings were conducted using CerePlex Direct data acquisition system (Blackrock), with a CerePlex u series Headstage (Blackrock). Electric stimulation was delivered using Isostim A320/A362 (World Precision Instruments) through Platinum Irridium concentric bipolar electrodes (0.2 Hz, 1 ms pulse width, 0.2 mA, FHC Inc). Optical stimulation was delivered using a 473 nm laser (Opto Engine LLC). Electric and optical stimulation were coordinated and programmed using a master 8 (AMP Instruments Ltd). Mice were anesthetized and placed into a stereotax. An optical fiber ferrule (Precision fiber products; OD 0.2mm, Thor labs), was implanted over the dorsal tip of the MR (A/P: −4.8, M/L: 0.0, D/V: −4.2) and cemented into place. The recording electrode (Neuronexus; A4×8-5mm-100-400-703-A32) was positioned in CA1 (A/P: −2.0, M/L: −1.0, D/V: fixed range −1.4 to −2.0) and held by a stereotactic arm. The stimulation electrode was lowered into CA3 at an angle to reach Schafer collaterals (A/P: −2.0, M/L: −3.0, D/V: variable range −1.6 to −2.5, angle: 27°) and held by a stereotactic arm. After at least 30 minutes of stable baseline recording, one train of optical stimulation was delivered (50 pulses, 20 Hz, 10 ms pulse width, 8 mW). Data were analyzed using Blackrock offline spike sorter, NeuroExplorer, and MATLAB.

Stereotaxic surgeries: 200um fiber optic implants were prepared using 1.25mm zirconia ferrules (Precision Fiber Products) with a 200um optical fiber (Thor Labs) as previously described (Yizhar et al., 2011).

Starting at 2 month of age, male and female mice and using standard stereotaxic procedures (Teixeira et al., 2006), fiber optic implants were bilaterally placed targeting the SLM-SR border of the CA1 region of the dorsal hippocampus (AP: 2.5, L: +/−2, DV: −1.6) or the outer blade of the DG (AP: 2.5, L: +/−2, DV: −2.0). Mice were allowed to recover for at least 2 weeks after surgery. For pCAV2-DIO-ZsGreen virus injections we targeted the SLM-SR border of the CA1 region of the dorsal hippocampus (Sanford et al., 2017). Virus microinjection was performed using Nanoject II (Drummond Scientific Nanoject II, Fisher Scientific, USA) attached to the guiding arm of the stereotaxic system. 50 nl deposits of pCAV2-DIO-ZsGreen tracer were pressure-injected five times in each of 3 dorsal-ventral coordinates (AP: 2.5, L: −2, DV: −1.6, −1.5, −1.4) for each mouse over 5 minutes using a glass micropipette (tip diameter of 25 μm). After the last injection, the needle was left in place for additional 15 minutes and then slowly withdrawn. After 3 weeks of post-surgery recovery, brains were analyzed for ZsGreen expression.

Behavioral testing: After recovery from surgery mice were subjected to a battery of tests performed in the following order: open-field (OF), social recognition (SR), water maze (WM) and forced-swim-test (FST). ChR2 and their respective controls were stimulated using blue light pulses (473 nm, 20 Hz, 10 ms, 10 mW). Arch and their respective controls were stimulated with green light continuously (532 nm, 10 mW).

The OF apparatus consisted of square Plexiglas activity chambers equipped with infrared detectors to track animal movement. Mice were allowed to walk freely over an 18-min trial. Optogenetic stimulation was presented in 3 min OFF, 3 min ON cycles. The time the mice spent in the center vs the time spent at the periphery of the arena, as well as the total distance traveled, were recorded. N(ChR2) = 16, $N(Control_{ChR2})$ = 17, N(Arch) = 14, $N(Control_{Arch})$ = 14. We removed one $Control_{Arch}$ mouse post-hoc from the OF analysis based on an outlier definition of being > 3 SD away from the mean.

The SR test was performed as described (Silverman et al., 2010). Briefly, mice were allowed to explore an arena with three sections for 5 min. Next, a mouse inside a wire container was placed on one side of the arena and an empty wire container in the other section. Mice were allowed to explore these containers for 10 min while being optogeneticaly stimulated or not. After this time, a novel mouse was placed in the empty container. The time the mice spent inspecting each of the containers was recorded for 10 min. N(ChR2) = 15, $N(Control_{ChR2})$ = 17, N(Arch) = 8, $N(Control_{Arch})$ = 8).

The apparatus and procedure for training in the WM was as previously described (Teixeira et al., 2006). Briefly, guided by extra-maze visual cues, mice were trained to find a submerged platform placed in a fixed location of the pool. On each of the 5 (non-implanted mice or ChR2 expressing group) or 9 (Arch expressing mice) training days, mice received three training trials. The order of the start locations was pseudo-randomly varied throughout training. The trial was complete once the mouse found the platform or when 60 s had

elapsed. When the mouse failed to find the platform in a given trial, it was guided onto the platform. Mice were optogeneticaly stimulated during the entire duration of training. During the probe test, the platform was removed, and the search pattern of the mouse was recorded for 60 s. In probe tests, we quantified performance by measuring the amount of time mice searched the target zone (17 cm in radius, centered on the location of the platform during training) versus the average of three other equivalent zones in other areas of the pool (Teixeira et al., 2006). These zones each represent ~5% of the total pool surface and a random search during the probe trial would be equivalent of 3 s in the area. CA1 placements: N(ChR2) = 8, N($Control_{ChR2}$) = 12, N(Arch) = 9, N($Control_{Arch}$) = 10. DG placements: N(ChR2) = 9, N($Control_{ChR2}$) = 17.

In the FST, mice were pre-exposed to a 5L beaker filled with warm water (27 °C) until the 3 l mark for 6 min. On the following day mice were placed in the same beaker for 18 min during which optogenetic stimulation was presented in 3 min OFF, 3 min ON cycles. Floating duration was quantified using View Point (ViewPoint Construction software). N(ChR2) = 15, N($Control_{ChR2}$) = 16, N(Arch) = 16, N($Control_{Arch}$) = 14.

Immunohistochemistry: For YFP, 5-HT, and Fos immunohistochemistry, mice were perfused transcardially with ice cold 0.1 M phosphate-buffered saline (PBS) and then 4% paraformaldehyde (PFA). For Fos-related experiments, mice were optically stimulated for 1 min at 20 Hz, 90 minutes prior to perfusion. Brains were removed, fixed overnight in PFA, and then transferred to a 30% sucrose solution and stored at 4°C. 50 μm coronal sections were cut and free-floating sections were prepared for immunohistochemistry. For immunodetection of 5-HT and YFP, sections were blocked for 2 h at room temperature (RT) with PBS-T containing 3% of bovine serum albumin (BSA; Sigma). Anti-GFP (rb, 1 :1000, Thermo Fischer Scientific) and Anti-5-HT (gt, 1 :500, Abcam) primary antibodies were incubated overnight at RT with PBS-T with 3% BSA. Sections were washed with PBS-T and then incubated for 2 h at RT with secondary antibodies (488 donkey anti-rabbit, 568 donkey anti-goat; 1 : 1000; Thermo Fischer Scientific). For immunodetection of 5-HT and Fos, sections were double immuno-labeled for 48 h at 4°C using goat anti-5HT (1:500; ab66047; Abcam) and rabbit anti-cFos (1:1000; Cell Signaling). Sections were washed with PBS-T and then secondary antibodies were applied to sections overnight donkey anti-goat Alexa 555 (1:1000; Thermo Fischer Scientific) and donkey anti-rabbit Alexa 647 (1:1000; Abcam). After subsequent washes with PBS-T, sections were mounted (Vectashield; Vectorlabs) and photographed using a Leica SP2 confocal microscope or Leica TCS SP8 microscope. Photographs were analyzed in Fiji. For Fos analysis, MR was contoured and the area was evaluated using the “measure” tool on the Fiji software. The numbers of Fos positive cell bodies co-localizing with 5-HT-immunoreactivity was counted with the GFP channel inactive and the experimenter blind to genotype. Number of neurons per MR area were normalized to ChR2-negative controls.

QUANTIFICATION AND STATISTICAL ANALYSIS

Statistical comparisons were performed using two-tailed parametric statistical tests, a one-tailed Student’s t-test (platform crossings), and repeated measures ANOVA followed by post hoc tests. Data are expressed as mean ± SEM.

Supplementary Material

Refer to Web version on PubMed Central for supplementary material.

Acknowledgement

We would like to thank Larry Zweifel for providing the pCAV2-DIO-ZsGreen virus. We thank Donald Wilson, Andrew Fink and Carl Edward Schoonover for their advice and help with setting up the *in vivo* electrophysiology system. This work has been supported by the National Institute of Mental Health (1R01MH113569 – 01, M.S.A), the Sackler Institute for developmental Psychobiology (M.S.A.), the Canada Research Chair in Developmental Cortical Physiology, and a Discovery Grant from the Natural Science and Engineering Research Council.

References and Notes

Ahmari SE, Spellman T, Douglass NL, Kheirbek MA, Simpson HB, Deisseroth K, Gordon JA, and Hen R (2013). Repeated cortico-striatal stimulation generates persistent OCD-like behavior. Science 340, 1234–1239. [PubMed: 23744948]

Almeida S, Glahn DC, Argyropoulos SV, and Frangou S (2010). Acute citalopram administration may disrupt contextual information processing in healthy males. Eur Psychiatry 25, 87–91. [PubMed: 19695841]

Andrade R (1998). Regulation of membrane excitability in the central nervous system by serotonin receptor subtypes. Ann N Y Acad Sci 861, 190–203. [PubMed: 9928257]

Bailey CH, Giustetto M, Huang YY, Hawkins RD, and Kandel ER (2000). Is heterosynaptic modulation essential for stabilizing Hebbian plasticity and memory? Nature reviews Neuroscience 1, 11–20. [PubMed: 11252764]

Basu J, and Siegelbaum SA (2015). The Corticohippocampal Circuit, Synaptic Plasticity, and Memory. Cold Spring Harb Perspect Biol 7.

Bockaert J, Claeysen S, Compan V, and Dumuis A (2011). 5-HT(4) receptors, a place in the sun: act two. Curr Opin Pharmacol 11, 87–93. [PubMed: 21342787]

Bockaert J, Sebben M, and Dumuis A (1990). Pharmacological characterization of 5-hydroxytryptamine4(5-HT4) receptors positively coupled to adenylate cyclase in adult guinea pig hippocampal membranes: effect of substituted benzamide derivatives. Mol Pharmacol 37, 408–411. [PubMed: 2314390]

Brun VH, Otnass MK, Molden S, Steffenach HA, Witter MP, Moser MB, and Moser EI (2002). Place cells and place recognition maintained by direct entorhinal-hippocampal circuitry. Science 296, 2243–2246. [PubMed: 12077421]

Brunelli M, Castellucci V, and Kandel ER (1976). Synaptic facilitation and behavioral sensitization in Aplysia: possible role of serotonin and cyclic AMP. Science 194, 1178–1181. [PubMed: 186870]

Cai X, Kallarackal AJ, Kvarta MD, Goluskin S, Gaylor K, Bailey AM, Lee HK, Huganir RL, and Thompson SM (2013). Local potentiation of excitatory synapses by serotonin and its alteration in rodent models of depression. Nature neuroscience 16, 464–472. [PubMed: 23502536]

Cohen JY, Amoroso MW, and Uchida N (2015). Serotonergic neurons signal reward and punishment on multiple timescales. Elife 4.

Cooke JD, Cavender HM, Lima HK, and Grover LM (2014). Antidepressants that inhibit both serotonin and norepinephrine reuptake impair long-term potentiation in hippocampus. Psychopharmacology 231, 4429–4441. [PubMed: 24781518]

Corradetti R, Ballerini L, Pugliese AM, and Pepeu G (1992). Serotonin blocks the long-term potentiation induced by primed burst stimulation in the CA1 region of rat hippocampal slices. Neuroscience 46, 511–518. [PubMed: 1545909]

Cowen P, and Sherwood AC (2013). The role of serotonin in cognitive function: evidence from recent studies and implications for understanding depression. J Psychopharmacol 27, 575–583. [PubMed: 23535352]

Dumuis A, Bouhelal R, Sebben M, Cory R, and Bockaert J (1988). A nonclassical 5-hydroxytryptamine receptor positively coupled with adenylate cyclase in the central nervous system. Mol Pharmacol 34, 880–887. [PubMed: 2849052]

Gray VC, and Hughes RN (2015). Drug-, dose- and sex-dependent effects of chronic fluoxetine, reboxetine and venlafaxine on open-field behavior and spatial memory in rats. Behav Brain Res 281, 43–54. [PubMed: 25523028]

Gruart A, Munoz MD, and Delgado-Garcia JM (2006). Involvement of the CA3-CA1 synapse in the acquisition of associative learning in behaving mice. The Journal of neuroscience : the official journal of the Society for Neuroscience 26, 1077–1087. [PubMed: 16436593]

Hitti FL, and Siegelbaum SA (2014). The hippocampal CA2 region is essential for social memory. Nature 508, 88–92. [PubMed: 24572357]

Hritcu L, Clicinschi M, and Nabeshima T (2007). Brain serotonin depletion impairs short-term memory, but not long-term memory in rats. Physiol Behav 91, 652–657. [PubMed: 17481676]

Huang YY, Pittenger C, and Kandel ER (2004). A form of long-lasting, learning-related synaptic plasticity in the hippocampus induced by heterosynaptic low-frequency pairing. Proc Natl Acad Sci U S A 101, 859–864. [PubMed: 14711997]

Hunt DL, Puente N, Grandes P, and Castillo PE (2013). Bidirectional NMDA receptor plasticity controls CA3 output and heterosynaptic metaplasticity. Nature neuroscience 16, 1049–1059. [PubMed: 23852115]

Ihara N, Ueda S, Kawata M, and Sano Y (1988). Immunohistochemical demonstration of serotonin-containing nerve fibers in the mammalian hippocampal formation. Acta anatomica 132, 335–346. [PubMed: 3057797]

Jahnsen H (1980). The action of 5-hydroxytryptamine on neuronal membranes and synaptic transmission in area CA1 of the hippocampus in vitro. Brain research 197, 83–94. [PubMed: 6249462]

Kandel ER, and Schwartz JH (1982). Molecular biology of learning: modulation of transmitter release. Science 218, 433–443. [PubMed: 6289442]

Kemp A, and Manahan-Vaughan D (2005). The 5-hydroxytryptamine4 receptor exhibits frequency-dependent properties in synaptic plasticity and behavioural metaplasticity in the hippocampal CA1 region in vivo. Cereb Cortex 15, 1037–1043. [PubMed: 15537670]

Kempadoo KA, Mosharov EV, Choi SJ, Sulzer D, and Kandel ER (2016). Dopamine release from the locus coeruleus to the dorsal hippocampus promotes spatial learning and memory. Proceedings of the National Academy of Sciences of the United States of America 113, 14835–14840. [PubMed: 27930324]

Lamirault L, and Simon H (2001). Enhancement of place and object recognition memory in young adult and old rats by RS 67333, a partial agonist of 5-HT4 receptors. Neuropharmacology 41, 844–853. [PubMed: 11684148]

Liu Z, Zhou J, Li Y, Hu F, Lu Y, Ma M, Feng Q, Zhang JE, Wang D, Zeng J, et al. (2014). Dorsal raphe neurons signal reward through 5-HT and glutamate. Neuron 81, 1360–1374. [PubMed: 24656254]

Madisen L, Mao T, Koch H, Zhuo JM, Berenyi A, Fujisawa S, Hsu YW, Garcia AJ, 3rd, Gu X, Zanella S, et al. (2012). A toolbox of Cre-dependent optogenetic transgenic mice for light-induced activation and silencing. Nature neuroscience 15, 793–802. [PubMed: 22446880]

Majlessi N, and Naghdi N (2002). Impaired spatial learning in the Morris water maze induced by serotonin reuptake inhibitors in rats. Behav Pharmacol 13, 237–242. [PubMed: 12122314]

Marchetti E, Dumuis A, Bockaert J, Soumireu-Mourat B, and Roman FS (2000). Differential modulation of the 5-HT(4) receptor agonists and antagonist on rat learning and memory. Neuropharmacology 39, 2017–2027. [PubMed: 10963745]

Matsukawa M, Ogawa M, Nakadate K, Maeshima T, Ichitani Y, Kawai N, and Okado N (1997). Serotonin and acetylcholine are crucial to maintain hippocampal synapses and memory acquisition in rats. Neurosci Lett 230, 13–16. [PubMed: 9259452]

Mendelsohn D, Riedel WJ, and Sambeth A (2009). Effects of acute tryptophan depletion on memory, attention and executive functions: a systematic review. Neuroscience and biobehavioral reviews 33, 926–952. [PubMed: 19428501]

Meneses A (2013). 5-HT systems: emergent targets for memory formation and memory alterations. Rev Neurosci 24, 629–664. [PubMed: 24259245]

Milner B, Squire LR, and Kandel ER (1998). Cognitive neuroscience and the study of memory. Neuron 20, 445–468. [PubMed: 9539121]

Mlinar B, Mascalchi S, Mannaioni G, Morini R, and Corradetti R (2006). 5-HT4 receptor activation induces long-lasting EPSP-spike potentiation in CA1 pyramidal neurons. Eur J Neurosci 24, 719–731. [PubMed: 16930402]

Nakashiba T, Young JZ, McHugh TJ, Buhl DL, and Tonegawa S (2008). Transgenic inhibition of synaptic transmission reveals role of CA3 output in hippocampal learning. Science 319, 1260–1264. [PubMed: 18218862]

Ogren SO, Eriksson TM, Elvander-Tottie E, D'Addario C, Ekstrom JC, Svenningsson P, Meister B, Kehr J, and Stiedl O (2008). The role of 5-HT(1A) receptors in learning and memory. Behav Brain Res 195, 54–77. [PubMed: 18394726]

Pastalkova E, Serrano P, Pinkhasova D, Wallace E, Fenton AA, and Sacktor TC (2006). Storage of spatial information by the maintenance mechanism of LTP. Science 313, 1141–1144. [PubMed: 16931766]

Penas-Cazorla R, and Vilaro MT (2015). Serotonin 5-HT4 receptors and forebrain cholinergic system: receptor expression in identified cell populations. Brain Struct Funct 220, 3413–3434. [PubMed: 25183542]

Restivo L, Roman F, Dumuis A, Bockaert J, Marchetti E, and Ammassari-Teule M (2008). The promnesic effect of G-protein-coupled 5-HT4 receptors activation is mediated by a potentiation of learning-induced spine growth in the mouse hippocampus. Neuropsychopharmacology 33, 2427–2434. [PubMed: 18075492]

Riad M, Garcia S, Watkins KC, Jodoin N, Doucet E, Langlois X, el Mestikawy S, Hamon M, and Descarries L (2000). Somatodendritic localization of 5-HT1A and preterminal axonal localization of 5-HT1B serotonin receptors in adult rat brain. J Comp Neurol 417, 181–194. [PubMed: 10660896]

Ropert N (1988). Inhibitory action of serotonin in CA1 hippocampal neurons in vitro. Neuroscience 26, 69–81. [PubMed: 2843792]

Rosen ZB, Cheung S, and Siegelbaum SA (2015). Midbrain dopamine neurons bidirectionally regulate CA3-CA1 synaptic drive. Nature neuroscience 18, 1763–1771. [PubMed: 26523642]

Rubio FJ, Ampuero E, Sandoval R, Toledo J, Pancetti F, and Wyneken U (2013). Long-term fluoxetine treatment induces input-specific LTP and LTD impairment and structural plasticity in the CA1 hippocampal subfield. Frontiers in cellular neuroscience 7, 66. [PubMed: 23675317]

Sanford CA, Soden ME, Baird MA, Miller SM, Schulkin J, Palmiter RD, Clark M, and Zweifel LS (2017). A Central Amygdala CRF Circuit Facilitates Learning about Weak Threats. Neuron 93, 164–178. [PubMed: 28017470]

Scott MM, Wylie CJ, Lerch JK, Murphy R, Lobur K, Herlitze S, Jiang W, Conlon RA, Strowbridge BW, and Deneris ES (2005). A genetic approach to access serotonin neurons for in vivo and in vitro studies. Proceedings of the National Academy of Sciences of the United States of America 102, 16472–16477. [PubMed: 16251278]

Silverman JL, Yang M, Lord C, and Crawley JN (2010). Behavioural phenotyping assays for mouse models of autism. Nature reviews Neuroscience 11, 490–502. [PubMed: 20559336]

Staubli U, and Otaky N (1994). Serotonin controls the magnitude of LTP induced by theta bursts via an action on NMDA-receptor-mediated responses. Brain research 643, 10–16. [PubMed: 7913394]

Suh J, Rivest AJ, Nakashiba T, Tominaga T, and Tonegawa S (2011). Entorhinal cortex layer III input to the hippocampus is crucial for temporal association memory. Science 334, 1415–1420. [PubMed: 22052975]

Sun Q, Srinivas KV, Sotayo A, and Siegelbaum SA (2014). Dendritic Na(+) spikes enable cortical input to drive action potential output from hippocampal CA2 pyramidal neurons. Elife 3.

Takeuchi T, Duszkiewicz AJ, Sonneborn A, Spooner PA, Yamasaki M, Watanabe M, Smith CC, Fernandez G, Deisseroth K, Greene RW, and Morris RG (2016). Locus coeruleus and dopaminergic consolidation of everyday memory. Nature 537, 357–362. [PubMed: 27602521]

Tanaka KF, Samuels BA, and Hen R (2012). Serotonin receptor expression along the dorsal-ventral axis of mouse hippocampus. Philos Trans R Soc Lond B Biol Sci 367, 2395–2401. [PubMed: 22826340]

Teissier A, Chemiakine A, Inbar B, Bagchi S, Ray RS, Palmiter RD, Dymecki SM, Moore H, and Ansorge MS (2015). Activity of Raphe Serotonergic Neurons Controls Emotional Behaviors. Cell Rep 13, 1965–1976. [PubMed: 26655908]

Teixeira CM, Pomedli SR, Maei HR, Kee N, and Frankland PW (2006). Involvement of the anterior cingulate cortex in the expression of remote spatial memory. The Journal of neuroscience : the official journal of the Society for Neuroscience 26, 7555–7564. [PubMed: 16855083]

Torres GE, Arfken CL, and Andrade R (1996). 5-Hydroxytryptamine4 receptors reduce afterhyperpolarization in hippocampus by inhibiting calcium-induced calcium release. Mol Pharmacol 50, 1316–1322. [PubMed: 8913363]

Tsien JZ, Huerta PT, and Tonegawa S (1996). The essential role of hippocampal CA1 NMDA receptor-dependent synaptic plasticity in spatial memory. Cell 87, 1327–1338. [PubMed: 8980238]

Varga V, Losonczy A, Zemelman BV, Borhegyi Z, Nyiri G, Domonkos A, Hangya B, Holderith N, Magee JC, and Freund TF (2009). Fast synaptic subcortical control of hippocampal circuits. Science 326, 449–453. [PubMed: 19833972]

Veerakumar A, Challis C, Gupta P, Da J, Upadhyay A, Beck SG, and Berton O (2014). Antidepressant-like effects of cortical deep brain stimulation coincide with pro-neuroplastic adaptations of serotonin systems. Biol Psychiatry 76, 203–212. [PubMed: 24503468]

Wang DV, Yau HJ, Broker CJ, Tsou JH, Bonci A, and Ikemoto S (2015). Mesopontine median raphe regulates hippocampal ripple oscillation and memory consolidation. Nature neuroscience 18, 728–735. [PubMed: 25867120]

Wawra M, Fidzinski P, Heinemann U, Mody I, and Behr J (2014). 5-HT4-receptors modulate induction of long-term depression but not potentiation at hippocampal output synapses in acute rat brain slices. PLoS One 9, e88085. [PubMed: 24505387]

Whitlock JR, Heynen AJ, Shuler MG, and Bear MF (2006). Learning induces long-term potentiation in the hippocampus. Science 313, 1093–1097. [PubMed: 16931756]

Yizhar O, Fenno LE, Davidson TJ, Mogri M, and Deisseroth K (2011). Optogenetics in neural systems. Neuron 71, 9–34. [PubMed: 21745635]

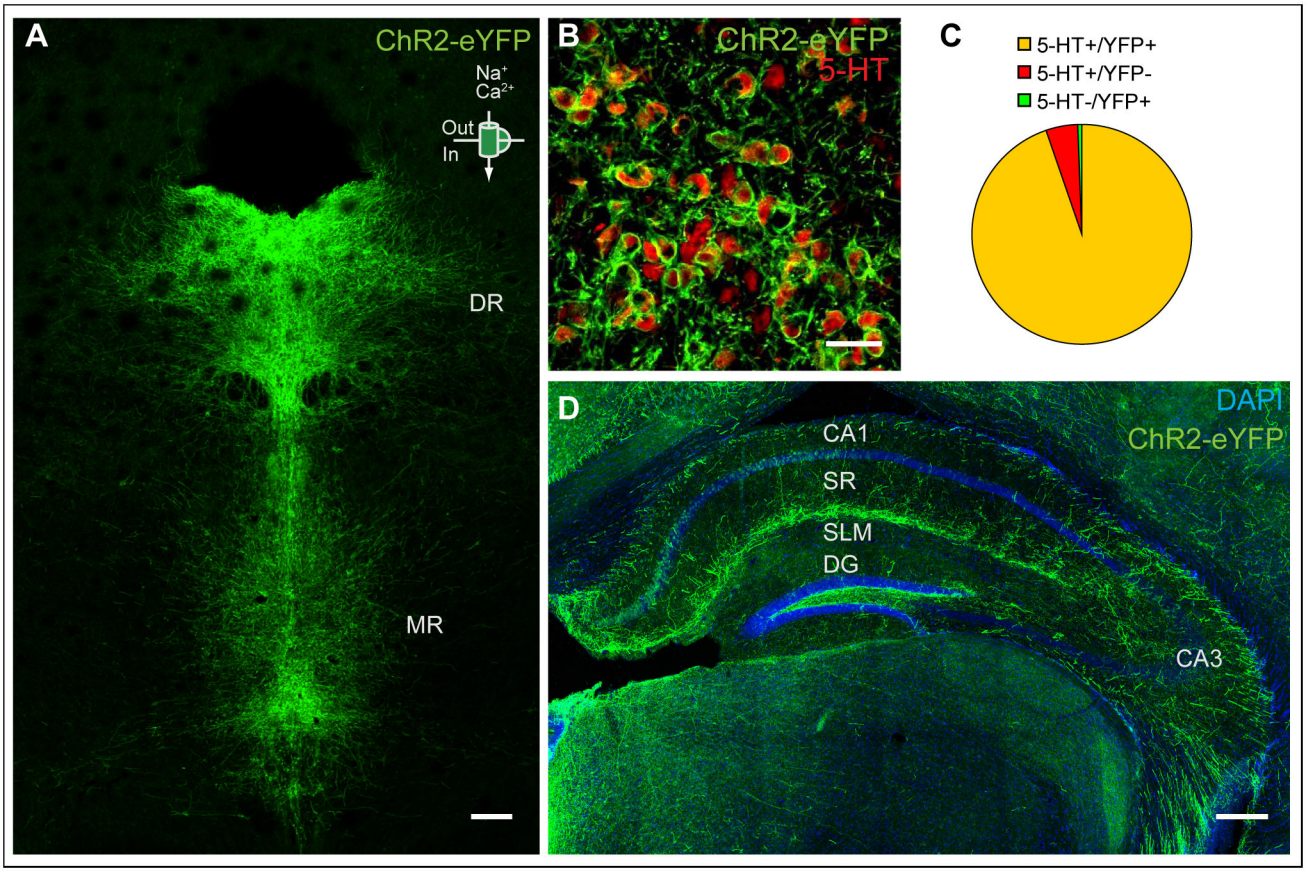

Figure 1: ChR2 expression in ePet1-cre;Ai32 mice.

(**a**) ChR2-YFP (green) is expressed throughout the raphe nucleus. DR- dorsal raphe, MR- medial raphe. Scale bar = 200 μm. (**b, c**) 94.8% of the cells analyzed co-stain for ChR2-YFP and 5-HT while 4.7% stain for 5-HT-only and 0.5% stain for ChR2-YFP-only. Scale bar = 50 μm (**d**) ChR2-YFP expression in the hippocampus. SR- stratum radiatum, SLM- stratum lacunosum moleculare, DG- dentate gyrus. Scale bar = 200 μm.

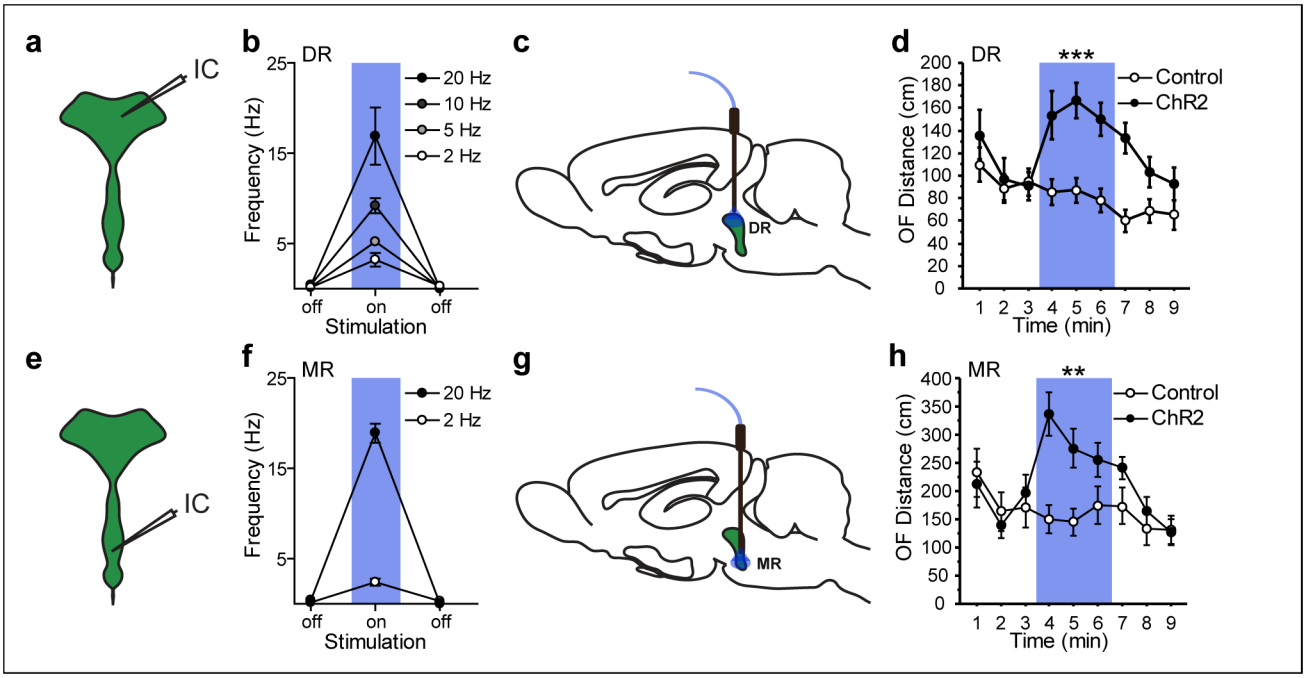

Figure 2: ChR2-based optogenetic stimulation of serotonergic neurons using ePet1-cre;Ai32 mice.

Schematic for intracellular recordings (IC) in raphe containing brain slices of serotonergic neurons in the DR (**a**) and MR (**e**). Relationship between the frequency of stimulation using 473 nm pulses of light and the firing frequency of ChR2-YFP expressing DR (**b**) and MR (**f**) cells in acute brainstem slices. Vertical blue shading indicates optogenetic stimulation. Schematic for *in vivo* photostimulation of serotonergic neurons in the DR (**c**) and MR (**g**). ePet1-cre;Ai32 mice displayed hyperlocomotion when stimulated using blue light in the DR (**d**) or MR (**h**) (blue band; 473nm, 10ms, 20Hz). Control: ePet1-cre$^{-/-}$;Ai32$^{+/+}$; ChR2: ePet1-cre$^{+/-}$;Ai32$^{+/+}$. Posthoc genotype effect in three minute light on block is indicated; **: $p < 0.01$, ***: $p < 0.001$.

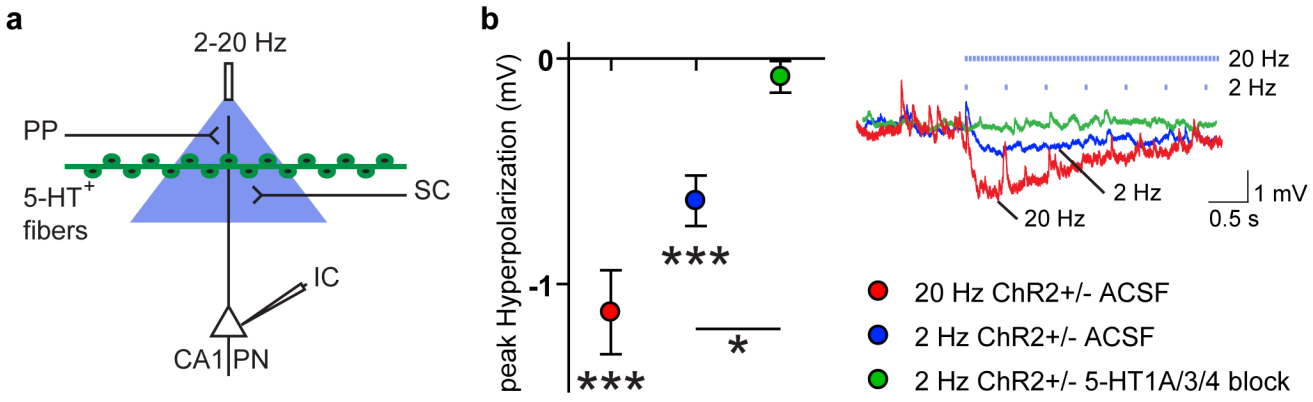

Figure 3: Optogenetic activation of serotonergic fibers in CA1 elicits a fast transient hyperpolarization of CA1 pyramidal neurons.

(**a**) Experimental configuration and circuit schematic. (**a-b**) 2 or 20 Hz optogenetic stimulation of ePet1-cre$^{+/-}$;Ai32$^{+/-}$ (ChR2$^{+/-}$) hippocampal slices induces a rapid hyperpolarization of CA1 pyramidal neurons. A cocktail of 5-HT receptor antagonists (GR113808, 100 nM; Odansetron, 10 nM; WAY100,635, 100 nM) blocked this hyperpolarization. Vm traces are taken from experiments representative of the population average. T-test based significant differences from baseline and between groups are indicated. *: $p < 0.05$, ***: $p < 0.001$.

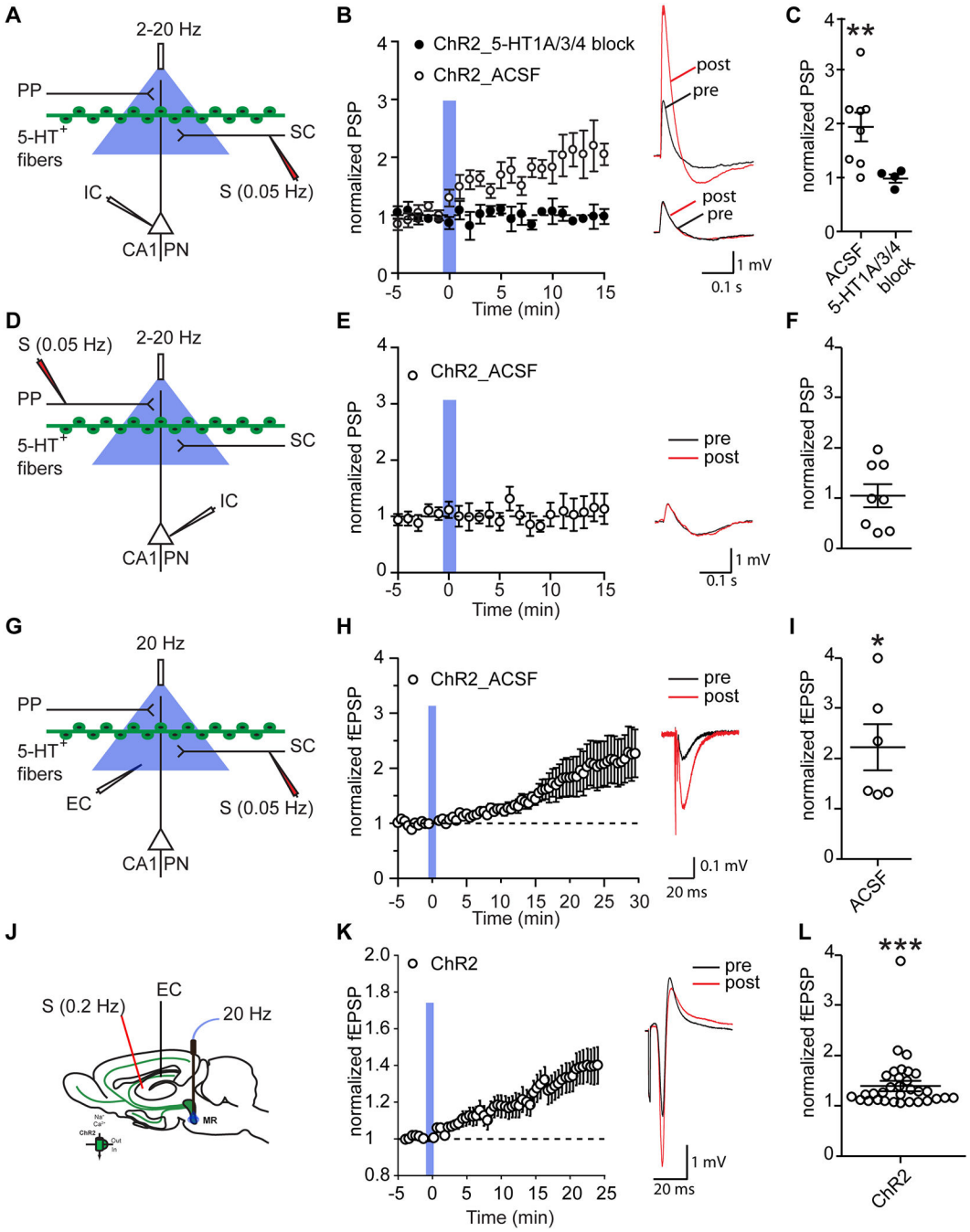

Figure 4: Optogenetic activation of serotonergic fibers in CA1 elicits a long-lasting potentiation of the CA3-CA1 synapse.

(**a, d, g, k**) Experimental configuration and circuit schematic. (**a-c**) When electrical stimulation of SR of CA1 at 0.05 Hz was paired with 50 blue light pulses (2 Hz), the PSP of CA1 pyramidal neurons increased. A cocktail of 5-HT receptor antagonists (GR113808, 100 nM; Odansetron, 10 nM; WAY100,635, 100 nM) blocked this potentiation of the CA3-CA1 synapse. (**d-f**) When the same protocol was applied to the perforant path we observed no potentiation. 2 Hz and 20 Hz experiments were averaged together because no effect of blue light stimulation frequency and no interaction between blue light stimulation frequency and

time was detected. (**g-i**) When electrical stimulation of SR of CA1 at 0.05 Hz was paired with 50 blue light pulses (20 Hz), and local field potentials were recorded extracellularly (EC), the fEPSP in CA1 was increased. (**k-m**) When electrical stimulation of SR of CA1 at 0.2 Hz was paired with 50 blue light pulses (20 Hz), and local field potentials were recorded *in vivo*, the fEPSP in CA1 was increased. (**b, e, h, l**) Vm traces are taken from experiments representative of the population average. Pre and 10 min post optogenetic stimulation traces are overlaid. Vertical blue shading indicates optogenetic stimulation. (**c, f, i, m**) Scatterplots show the normalized PSP 10 – 15 minutes after optical stimulation (**c, f**), the normalized fEPSP 25 – 30 minutes after optical stimulation in slices (**i**), and the normalized fEPSP 20 – 25 minutes after optical stimulation *in vivo* (**m**). T-test based significant differences from baseline and between groups are indicated. *: $p < 0.05$, **: $p < 0.01$, ***: $p < 0.001$.

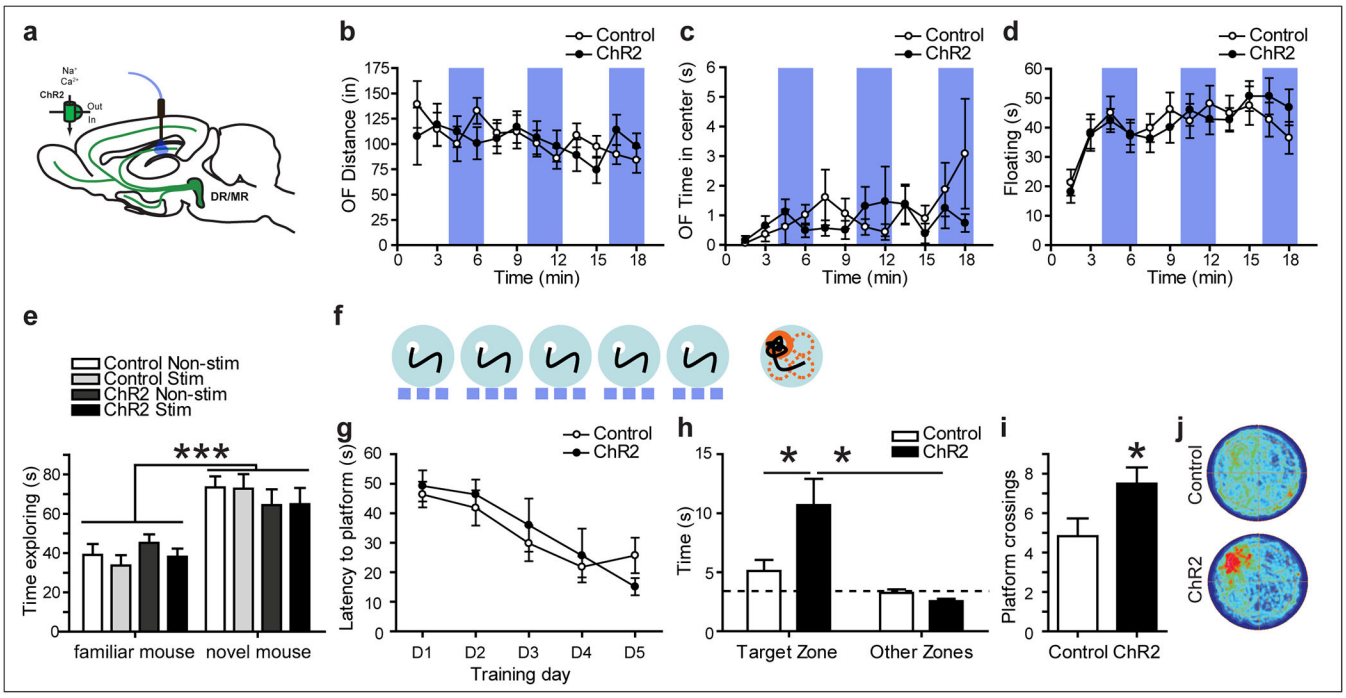

Figure 5: Optogenetic activation of serotonergic terminals in CA1 increases water maze memory formation.

(**a**) Experimental design for stimulating CA1 5-HT release *in vivo*. No differences between genotypes and no effect of light stimulation was found on locomotion (**b**), time in the center in the OF (**c**), floating in the FST (**d**) or social recognition (**e**). Vertical blue shading indicates optogenetic activation of ChR2. (**f-g**) In the water maze, mice were trained for 5 days, 3 trials per day while stimulated with blue light at 20 Hz (blue dashes). (**g**) No effect of stimulation was detected during training. (**h**) During a 60s probe trial, ChR2-expressing mice spent more time in the zone where the platform was previously located (Target zone) than ChR2-non-expressing littermate control mice. The dashed line indicates random search. (**i**) ChR2 expressing mice crossed the area where the platform was previously located more often. (**j**) Density plots of probe trial behavior. Control: ePet1-cre$^{-/-}$;Ai32$^{+/+}$; ChR2: ePet1-cre$^{+/-}$;Ai32$^{+/+}$. *: $p < 0.05$, ***: $p < 0.001$.

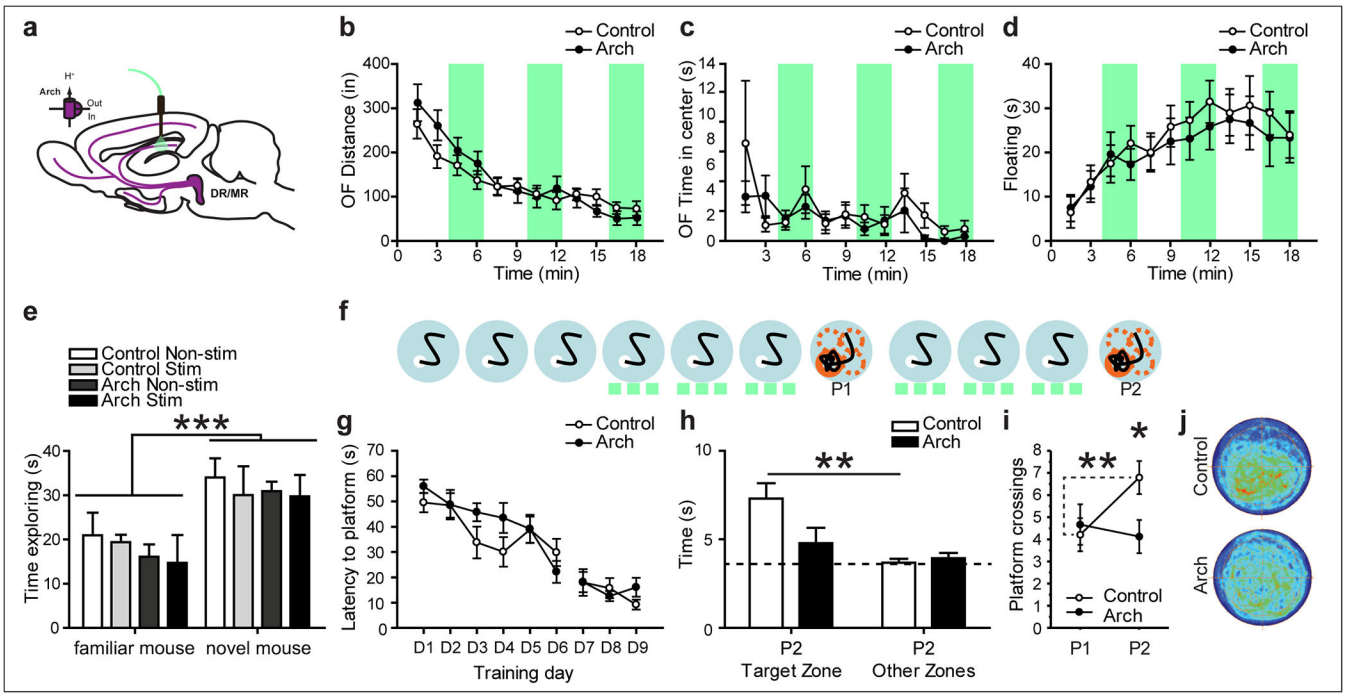

Figure 6: Optogenetic inhibition of serotonergic terminals in CA1 impairs water maze memory formation.

(**a**) Experimental design for inhibiting CA1 5-HT release *in vivo*. No effect of genotype or light was found on locomotion (**b**), time in the center in the OF (**c**), floating in the FST (**d**) or social recognition (**e**). Vertical green shading indicates optogenetic activation of Arch. (**f-g**) Mice were trained in the water maze for 6 days, 3 trials per day, given a first probe trial (P1), followed by 3 additional days of training and tested again in a second probe trial (P2), with green light administered as indicated (green dashes). (**g**) No effect of stimulation was detected during training. On P2 Arch expressing mice spent less time in the target zone (**h**) and crossed the platform area less times (**i**) than their non-expressing controls. (**j**) Density plots of P2 behavior. Control: ePet1-cre$^{-/-}$;Ai35$^{+/+}$; Arch: ePet1-cre+/−;Ai35$^{+/+}$. *: $p < 0.05$, **: $p < 0.01$, ***: $p < 0.001$.

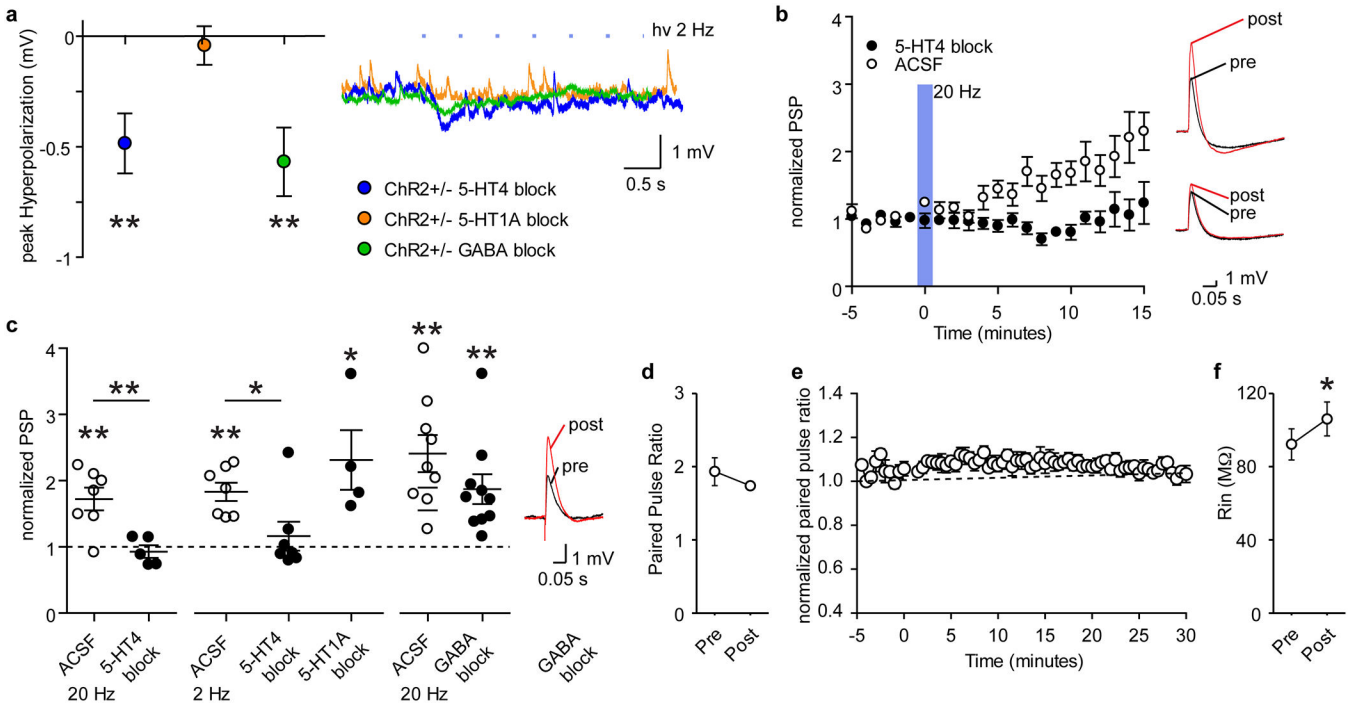

Figure 7: 5-HT4R-mediated modulation of hippocampal plasticity.

(**a**) 5-HT1AR antagonism (WAY100635, 100 nM) but not 5-HT4R antagonism (GR113808, 100 nM) or GABA receptor antagonism (SR-95531, 2 μM and CGP-35348, 1 μM) blocked the fast-transient hyperpolarization after optogenetic stimulation of serotonergic terminals in CA1. ChR2$^{+/-}$: ePet1-cre$^{+/-}$;Ai32$^{+/-}$. (**b-c**) 5-HT4R but not 5-HT1AR antagonism or GABA receptor antagonism blocked the potentiation of the CA3-CA1 synapse after optogenetic stimulation of serotonergic terminals in CA1 at either 2Hz or 20Hz. (**c**) Scatterplot shows the normalized PSP 10–15 minutes after optical stimulation. (**d, e**) Paired pulse ratio was not altered by optogenetic stimulation in either intracellular (**d**) or extracellular (**e**) slice recordings. (**f**) Input resistance (Rin) was increased after optogenetic stimulation. T-test based significant differences from baseline and between groups are indicated. *: $p < 0.05$, **: $p < 0.01$.

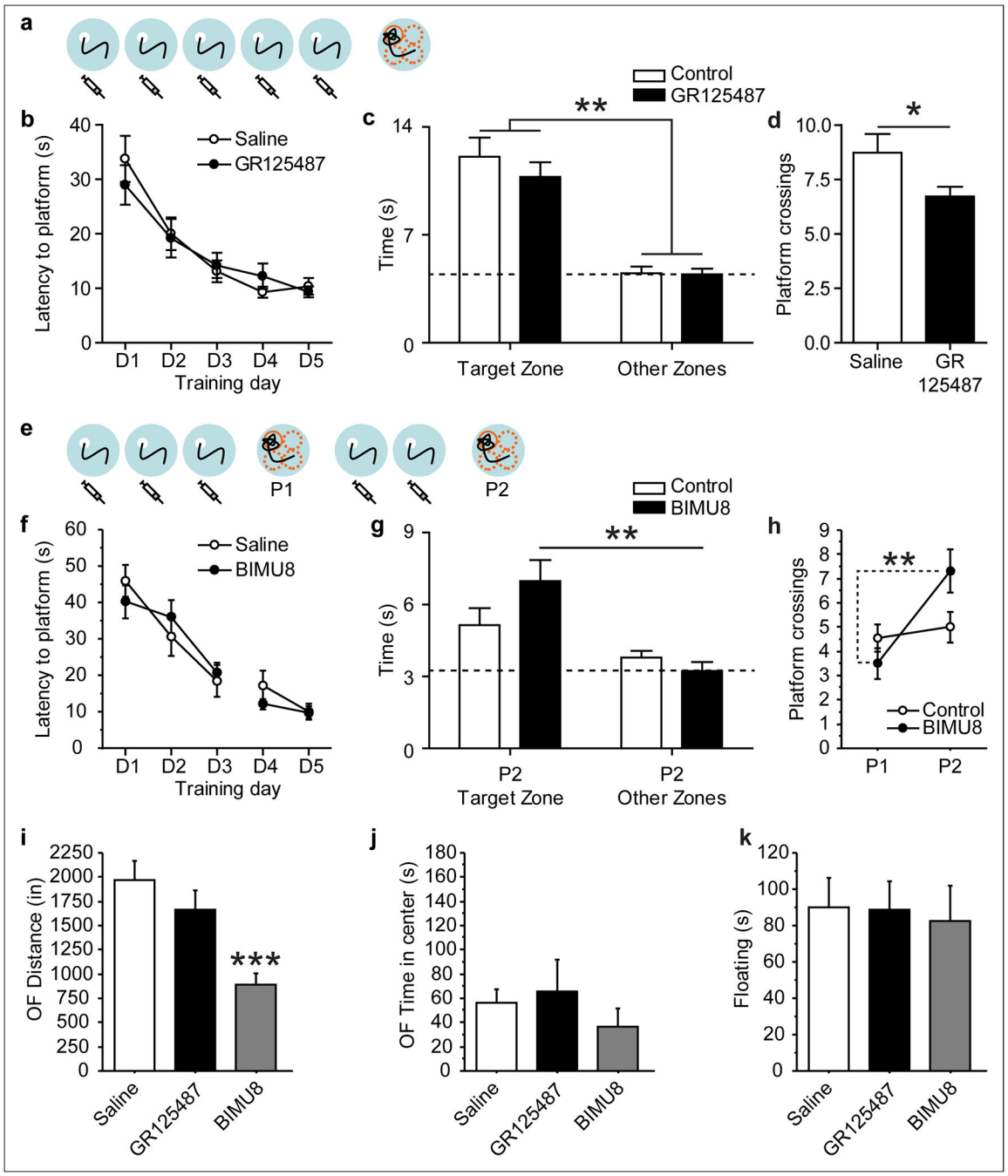

Figure 8: Bidirectional modulation of water maze memory through pharmacological 5-HT4 receptor interference.

Mice were assessed in the MWM (**a-h**), OF (**i-j**) and FST (**k**). (**a, b**) Mice were treated with the 5-HT4 receptor antagonist GR125487 or with saline vehicle for 5 days, 20 min before water maze training. (**c**) During probe trial, no effect of treatment was detected for zone times, but (**d**) GR125487 injected mice crossed the platform area significantly fewer times. (**e, f**) Mice were treated with the 5-HT4 receptor agonist BIMU8 or with saline vehicle for 5 days, 20 min before water maze training. Probe trial performance was significantly improved

in BIMU8 injected mice, which spent more time in the target zone on P2 (**g**) and crossed the platform location more often (**h**) than saline injected Controls. (**i-k**) Mice were treated with GR125487, BIMU8 or Saline 20 min before testing. BIMU8 treatment reduced ambulatory activity in the OF, while GR125487 had no effect (**i**). No effect of treatment was detected for OF center time (**j**) or FST floating time (**k**). *: $p < 0.05$, **: $p < 0.01$, ***: $p < 0.001$.